A Large-Scale Model Experiment on the Effect of Sheet Pile Wall on Reducing the Damage of Oil Tank Due to Liquefaction

Nanase OGAWA
Chief, Construction Solutions Department, GIKEN LTD., Tokyo, Japan
Email: ogawa@giken.com
Yukihiro ISHIHARA
Manager, Press-in Technologies Support Department, GIKEN LTD., Tokyo, Japan
Email: ishihara@giken.com
Katsuhiko ONO
Manager, Construction Solutions Development Department, GIKEN LTD., Tokyo, Japan
Masanori HAMADA
Professor emeritus, Waseda University, Tokyo, Japan

ABSTRACT

After the Alaska Earthquake and the Niigata Earthquake in 1964, many researches have been conducted on the liquefaction and its caused damage. In the 2011 Great East Japan Earthquake, liquefaction of sandy ground was observed in wide areas. The authors have built a large-soil tank for the experiment to develop effective liquefaction countermeasures. The soil box can cause and keep the liquefaction continuously by injecting the water flow from the bottom of the model ground. This paper introduces this experimental apparatus and reports one of the test results on the behaviour of the oil tanks during liquefaction and the effectiveness of the measures by using sheet pile walls.

Key words: *Liquefaction, Large-scale model experiment, Seepage force, Oil tank, Sheet pile wall*

1. Introduction

According to Sangawa (2008), due to the spread of earthquake archaeology, many traces of liquefaction have been discovered by excavation investigations. It has been proven in Japan, that many cases of liquefaction have taken place from long before. In the study by Kusano *et al*. (1989), information on liquefaction was scarce at the time of the Great Kanto Earthquake in 1923, since the disaster due to fires was enormous. However, they reported that liquefaction did occur in the wide Kanto area. Following this, after the Fukui Earthquake in 1948, studies on liquefaction by Mogami *et al*. (1953) began, and many researches on liquefaction have conducted after the Niigata Earthquake and the Alaska Earthquake in 1964 which caused heavy liquefaction damages (Yasuda 1988).

At the time of the Great East Japan Earthquake in 2011, liquefaction occurred in wide areas of the east Japan. As a cause of liquefaction, duration of earthquake ground motion is pointed out, together with the intensity of the motion. In the Hyogo-ken Nanbu Earthquake in 1995 and the Kumamoto Earthquake in 2016, a maximum acceleration was recorded 5 seconds after the ground began to quake, and the ground motion ceased in the next 10 to 20 seconds. On the other hand, the quake of the Great East Japan Earthquake in 2011 showed a maximum acceleration 20 seconds after the initial quake, and it lasted more than 150 seconds. Many people may still have a clear image of the occurrence of sand boils in reclaimed lands along the Tokyo Bay coast and damages in the form of tilted buildings due to differential settlements, since they were broadcast by many media. The economical damage due to liquefaction became a record making incident.

At auhors, a liquefaction generator was built to develop liquefaction countermeasures using piles and

sheet piles, and to clarify the characteristics of pile and sheet pile structures in liquefied grounds. This paper presents the characteristics of the liquefaction generator and an experimental result on the effect of liquefaction countermeasures for oil tanks.

2. Outline of liquefaction generator

2.1. Development concept

Shaking table and dynamic centrifugal experiments have been carried out to simulate liquefaction phenomenon in the ground. In these experimental apparatuses, the size of the experimental models is limited by the dimensions of soil tanks that can be installed on the shaking table. The model scales of 1:10 to 1:50 have been often used (*e.g.*, The Japanese Geotechnical Society 1994, Tani 2013). The stress state is simulated by taking into account the strain dependency of the ground properties in the shaking table experiments, while it is simulated using the centrifugal force corresponding to the reduction scale of the model is considered in the dynamic centrifugal experiments (Hayashi 1997). There is an advantage in either case that the experiments can be repeated relatively easily, since a contracted small model is used in the experiments. However, small model have drawbacks such as selection of materials and constraints on measurement points. Therefore, the similarity in the experiments has to be increased, using as large a model as possible. From the viewpoints of time and cost required to build the model, it may be said that there might be a compromise necessary to some extent.

The authors have developed liquefaction countermeasures by driving piles and sheet piles that are effective and easy to use in construction into liquefiable grounds. They have also developed an experimental apparatus that can simulate the behaviour of the developed countermeasures against the occurrence of liquefaction.

The followings are concepts for the development of experimental apparatus;

1) The experiment apparatus should be able to accommodate models in dimensions close to the full-scale piles/sheet piles, so that the construction efficiency may be studied; and
2) It should be able to accommodate vertical and horizontal loading tests (Japan Geotechnical Society (JGS) 2002 and 2010) to verify behaviours of piles and structures in the liquefied ground.

As a result, a soil tank was developed that could simulate constructions of recently popular 1,000 mm diameter steel tubular piles, and also could accommodate pile loading tests. From the standard on the influence range of pile loading test, the tank built had a dimension of 7 m x 7 m cross-section with a depth of 9 m (**Fig. 1**).

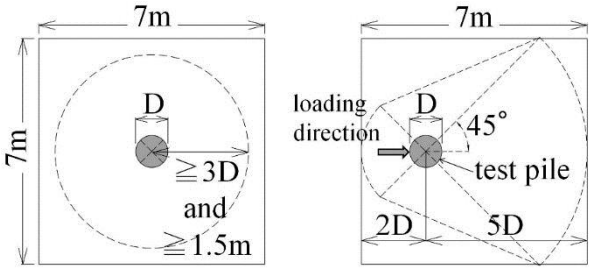

a) vertical load test b) horizontal load test

Fig. 1 The influenced area of test pile (JGS 2002&2010)

2.2. Reproductive method of liquefaction

Liquefaction phenomenon of the ground induced by earthquake ground motion is explained as shown in **Fig. 2 (a)**. When shear force due to earthquake acts in the ground that is loosely piled up below the groundwater level, contacts between soil particles are lost, and the particles tend to move in the sedimentation direction due to gravity. Liquefaction is a state where soil particles in a sequential change completely float in the pore water, and effective stress becomes zero. At this state, since the surcharge load that was carried and transmitted through the soil particles is now born by the pore water pressure, and then pore water pressure increases. After the seismic motion ceases, discharge of pore water and soil particle sedimentation continue, and the contacts between the soil particles are restored. Besides the vibration of the ground, the liquefaction status can be caused by the upward seepage of the ground water, as shown in **Fig. 2 (b)**. When upward seepage pressure acts on the soil particles due to upward water flow, contacts between the soil particles are lost, and the particles become in a state of floating in pore water and effective stress of the soil is lost. In this method, when the upward seepage flow ceases, soil particles start to pile up, and effective stress is restored.

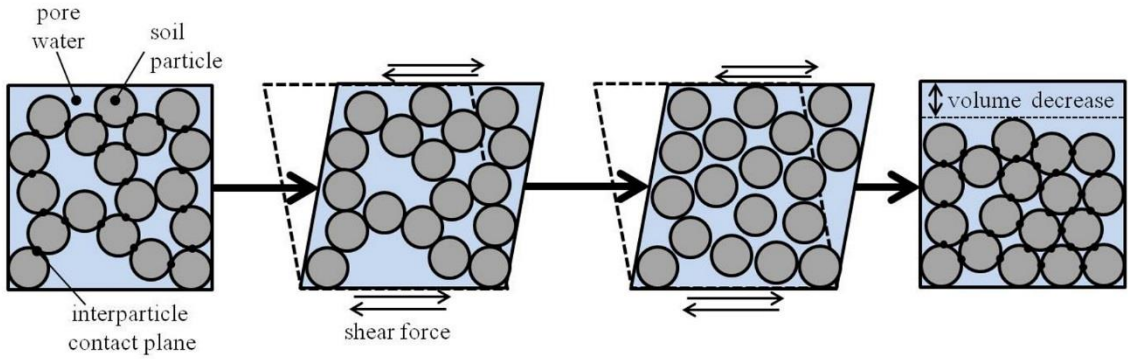

[i] before liquefaction [ii] shear deformation [iii] liquefaction [iv] after liquefaction

a) The state variation of sandy soil caused by shear deformation

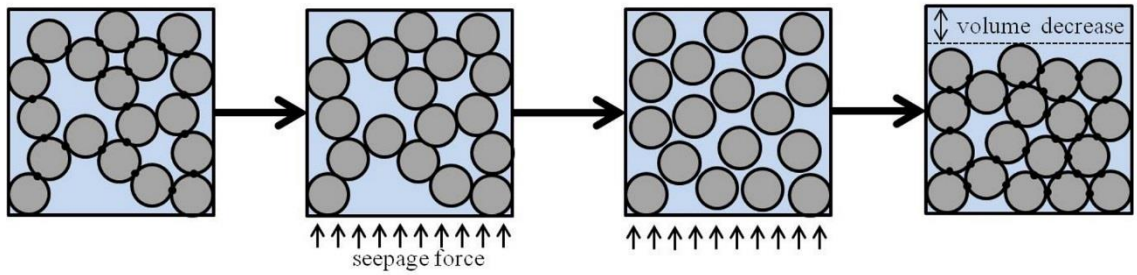

[i] before liquefaction [ii] upward seepage flow [iii] liquefaction [iv] after liquefaction

b) The state variation of sandy soil caused by upward seepage flow

Fig. 2 The liquefaction mechanism (as in Ishihara (1998))

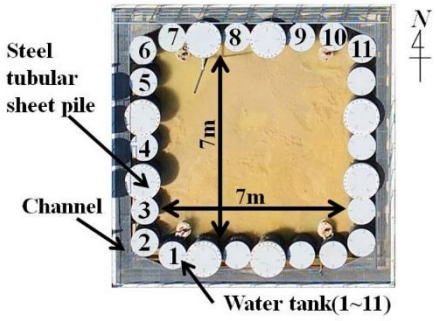

Steel tubular sheet pile(s) : The wall of soil tank is made from 26 no. tubular piles of 1000mm diameter. It is 7m square cross section and 9m depth.
Water tank : The water reservoir tank, 11 no. Water tank utilize the inside of the tubular piles for the walls.
Drainage channel : The drainage channel was provided so that the water overflowing from the soil tank into the water reservoir tank again.

a) Plan view

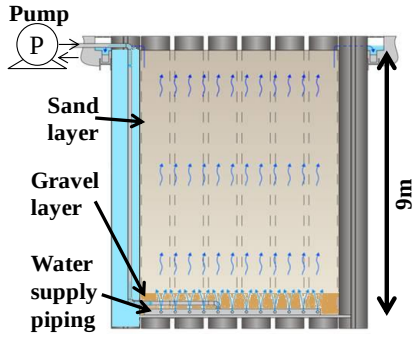

Water supply piping : Water in the water reservoir tank has supplied from the bottom of the soil tank to generate upward seepage flow.
Gravel layer : Material for providing a gap installed around the supply piping so that the water pressure distribution in the soil tank rises uniformly.
Sandy layer : Single sand ground consisting of artificial material with controlled grain size distribution.

b) Cross section view

Fig. 3 Plan view and cross section view of tank

2.3. Structure of equipment

As shown in **Fig. 3**, the experiment apparatus consists of a soil tank by steel tubular sheet piles (hereafter tubular piles), a water reservoir tank utilizing the inside of the tubular piles, and a piping to generate upward seepage flow from the bottom of the soil tank. The soil tank was built in such a way that a rectangular earth retaining wall with an inner dimension of 7 m x 7 m was first built using 26 tubular piles of diameter 1000mm, and the bottom slab was installed after the inner soil was excavated, and the inner space was filled with sand. 26 tubular piles, 11 out of which are numbered, were connected to build an earth retaining wall for a water

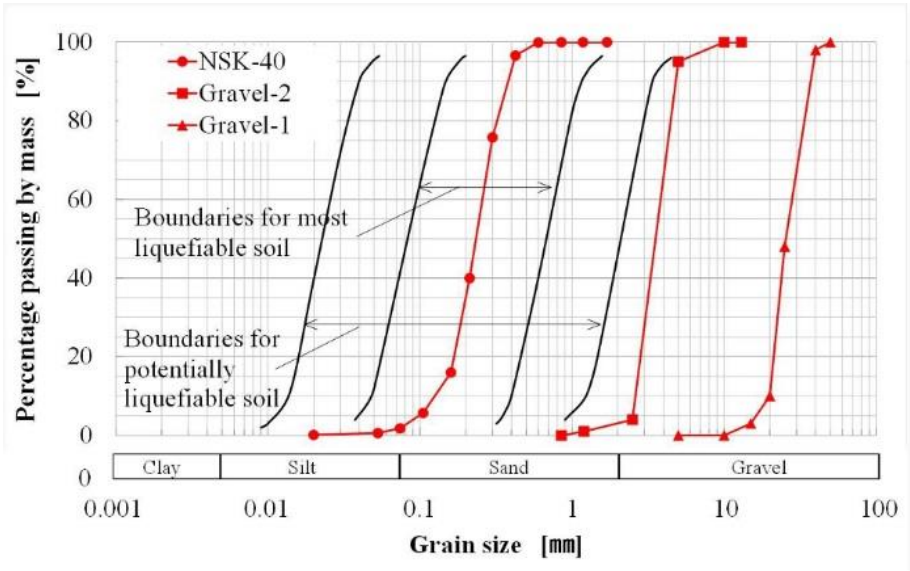

Fig. 4 The grain size distribution curves

reservoir tank and has a total capacity of about 70 m^3 (**Fig. 3 a)**). Since a large volume of water is required to maintain the liquefaction state for several tens of minutes, an open channel was installed on the upper rim of the soil tank so that the water filled in the water reservoir could be circulated.

An incline was given to the open channel, so the overflown water could flow into Nos.1 and 11 tubular piles. The water that flowed into the two tubular piles is collected in No. 6 tubular piles and pumped up from the bottom of the soil tank. The water that flowed inside the ground reached the ground surface, and flowed into the open channel and returned back to the reservoir tank. Repeating these stages, upward seepage flow can be generated continuously and liquefaction state can be continued for a certain amount of time.

A filter layer by gravel was installed to make the water flow uniform, and to prevent sand particles from flowing into the water supply piping through the holes prepared along the piping (**Fig. 3 b)**).

3. Soil property

3.1. Model ground

The sand for the experiment was selected in such a way that it would take some time for pore water pressure to dissipate and was easily commercially available in large amounts, among those described in The Ports & Harbours Association of Japan (2007), especially from ones with a grain size distribution at which liquefaction possibility was high. The grain size distribution of the selected Shimane sand (NSK-40) is shown by the solid circles, while those of the gravel filter materials are shown by solid squares and solid triangles in **Fig. 4**. In selecting the filter materials, the concept of zone type filters used in the design of rockfill dams by Ohne (2006) was referred to. After installing the pipe channel, a 200 mm thick Gravel-1 layer with an average particle size of 25 mm was set, followed by a 100 mm thick Gravel-2 layer with an average particle size of 3.5 mm, and finally the layer of NSK-40 with an average particle size of 0.31 mm. **Table 1** shows physical properties of NSK-40.

Table 1. Physical properties of soil (NSK-40)

Soil particle density	ρ_s	g/cm^3	2.64
Maximum void ratio	e_{max}		0.909
Minimum void ratio	e_{min}		0.552
Coefficient permeability	k	cm/s	2.36×10^{-2}
Wet unit weight	γ_t	kN/m^3	19.2
Void ratio	e		0.719
Relative density	D_r	%	53

3.2. Relationship between the water discharge and excess pore water pressure ratio

The liquefaction state of the ground is one in which pore water pressure supports the surcharge load that had been supported by the soil particle contacts. It may be seen that the pore water pressure is zero at the ground surface,

and an upward seepage flow is generated by the water head difference caused by the occurrence of excess pore water pressure. The velocity of the seepage flow in the soil v is given by the permeability k and a hydraulic gradient i by the Darcy's law in **Eq. (1)**.

$$v = k \cdot i \tag{1}$$

The hydraulic gradient at which soil particles become into a floating condition is termed the critical hydraulic gradient, and is given by **Eq. (2)**,

$$i_{cr} = \frac{G_s - 1}{1 + e} \tag{2}$$

where G_s is the specific gravity of the soil particle and e is the void ratio. When $i \geqq \alpha\ i_{cr}$, liquefaction takes place. Yamashita *et al*. (1981) carried out one-dimensional permeability test, and presented a correction factor α using Kyudai sand and Toyoura sand (**Fig. 5**), comparing the measured critical hydraulic gradient obtained from the state at which sand boil was confirmed by eye observation with the value obtained using **Eq. (2)**.

Based on this, an experiment was conducted to verify the correction factor α of NSK-40 using a small soil tank shown in **Fig. 6**. Water was supplied through the holes prepared in the bottom slab of the soil tank, and an upward seepage flow was generated through the gravel layers. The

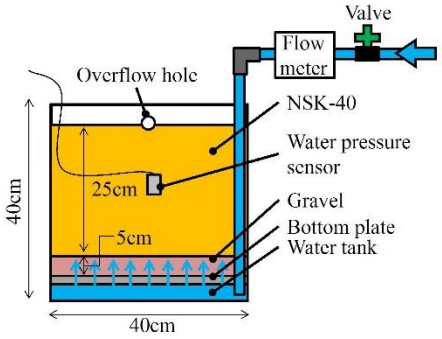

Fig. 6 Model test of liquefaction system

amount of supplied water and the pore water pressure in the sand layer were measured. Note the sand layer was prepared with a relative density of 53 %. In **Fig. 7**, flow rate Q is plotted against the excess pore water pressure ratio r_u. As shown in **Eq. (3)**, r_u is the ratio of the excess pore water pressure Δu to the effective stress σ'_{v0}.

$$r_u = \frac{\Delta u}{\sigma'_{v0}} \tag{3}$$

The flow rate Q at $r_u = 1$ was taken as the flow rate at the occurrence of liquefaction. Substituting **Eq. (1)** and the coefficient of Yamashita *et al*. into **Eq. (4)** used to calculate the amount of water supplied, α was calculated using **Eq. (5)**,

$$Q = v \cdot A \tag{4}$$

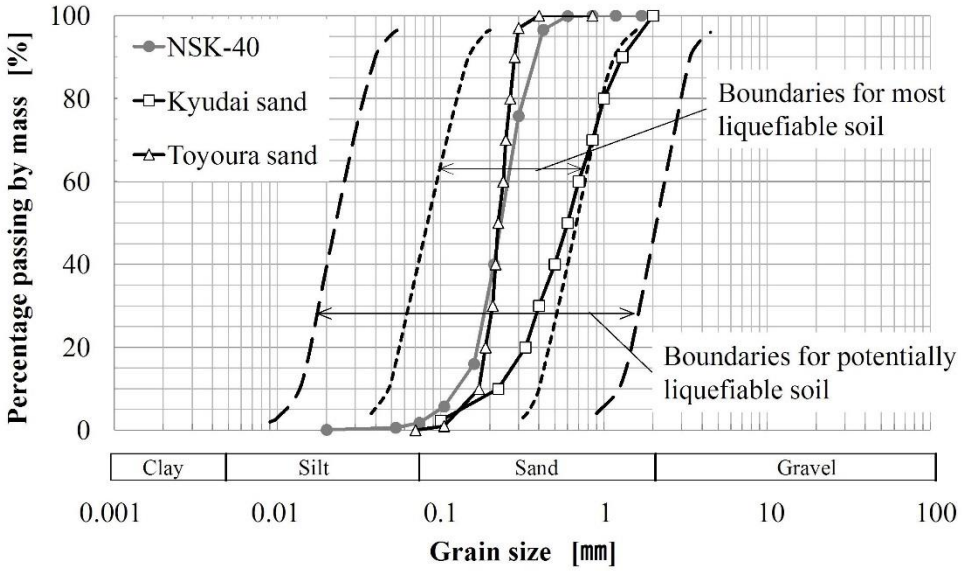

Fig. 5 The gradation curves for preliminarily tests
(Add with Uchida(1981))

$$= \alpha \cdot k \cdot i_{cr} \cdot A \quad (5)$$

where Q is the amount of water, A is the cross-section of the soil tank and α is the correction factor for the critical hydraulic gradient. **Fig. 8** shows the results of the small-scale model experiments added to the calculated correction factor α and the experimental results by Yamashita *et al*. (1981). Note that the correction factor α was calculated based on the uniformity coefficient U_c of NSK-40, since there was correlation between U_c and α. With this, amount of water necessary to cause liquefaction Q_{est} was estimated to be 1.35m^3/min. from **Eq. (5)**.

Based on these results, Q and r_u were verified using the model ground prepared in the large soil tank. **Fig. 9** depicts Q, r_u and estimated Q_{est}. Four water pressure sensors were installed at depths of 0.5, 2.5, 4.5 and 6.5 m from the surface of the soil layer. The change in water pressure was measured, generating upward seepage flow. At a depth of 0.5 m, r_u abruptly changed and it reached unity right after the beginning of the measurement. This results from variable unit weight of the ground near the ground surface, since the phreatic surface of the seepage flow became 0.3 m higher than the ground surface of the model ground. The value of r_u increased with the increase in Q, and it was verified the ground at depths shallower than 6.5 m liquefied when Q was about 1.3m^3/min. Considering an average value of Q for the entire soil layer, Q_{est} is on the approximate line at a depth of 6.5 m, suggesting that the average behaviour of the soil layer can be represented by the relationship shown in **Fig. 8**. Moreover, as shown in **Fig. 10**, it was verified that r_u in the ground could be maintained constant, if the amount of supply water was kept constant.

3.3. Assumption of seismic ground motion

For the judgement of ground liquefaction, the liquefaction resistance factor F_L has been used in many guidelines including the Specifications for Highway Bridges (Japan road association (2017)). F_L is the ratio of dynamic shear strength ratio R to the seismic shear stress ratio L (**Eq. (6) – (8)**). The ground is judged to liquefy when $F_L \leq 1$. **Fig. 11** shows the relationship between the value of F_L in the model ground and the horizontal acceleration on the ground surface.

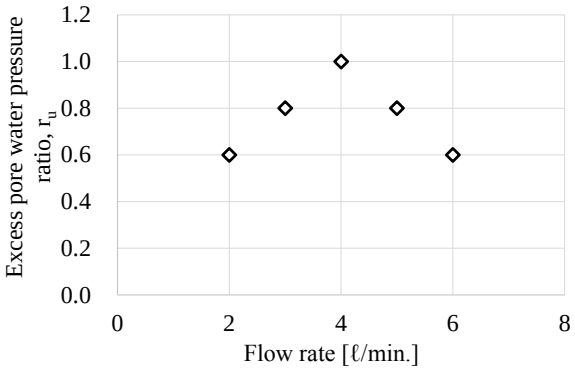

Fig. 7 Relationship between flow rate and excess pore water pressure (using **Fig.6** tank)

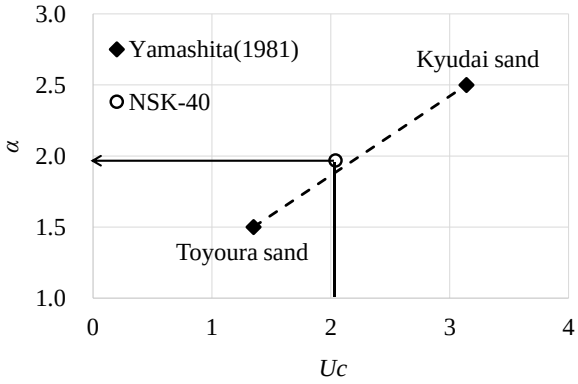

Fig. 8 Factor of critical hydraulic gradient

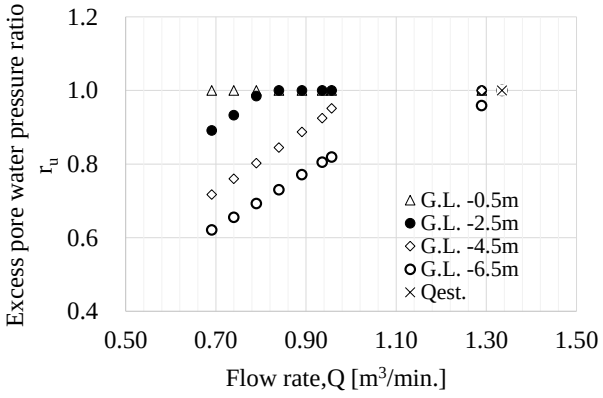

Fig. 9 Relationship between flow rate and excess pore water pressure (using **Fig. 3** tank)

$$F_L = R / L \quad (6)$$

$$R = c_W \cdot R_L \quad (7)$$

$$L = r_d \cdot k_{hgL} \cdot \sigma_v / \sigma'_v \quad (8)$$

Here, c_w is modification factor on earthquake

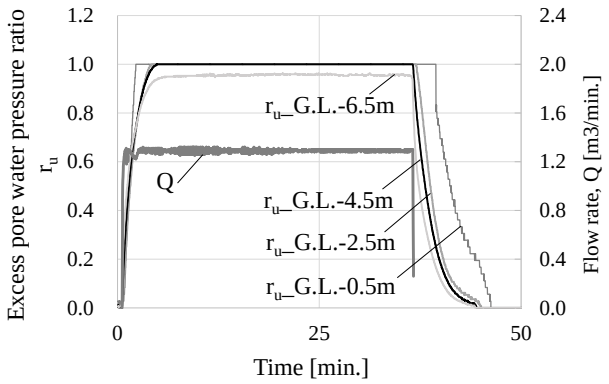

Fig. 10 An example of time relationship between r_u and Q

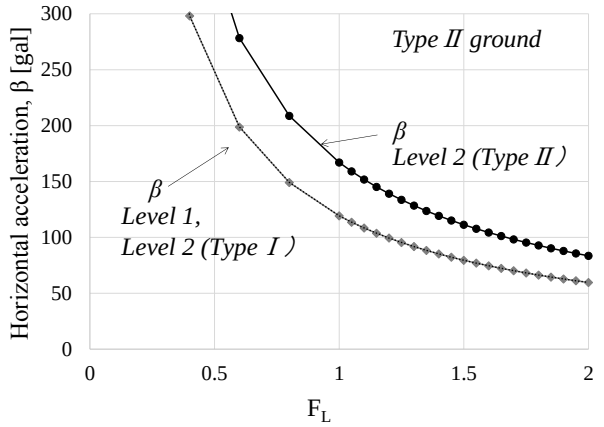

Fig. 11 Relationshop beween F_L and horizonal acceleration (Japan road association (2017))

Photo 1. Inclination and subsidence of tanks (Hamada, 2011)

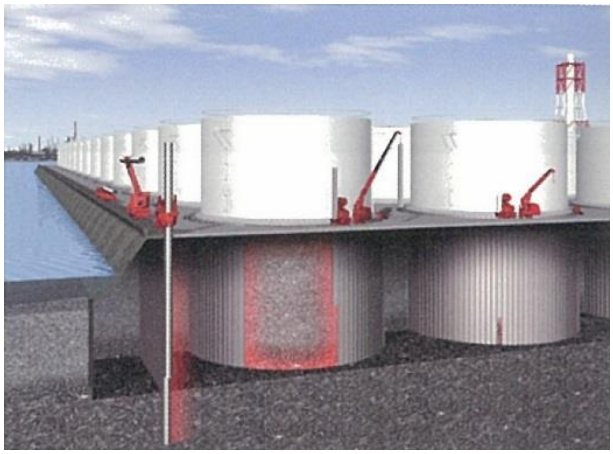

Fig. 12 Sheet pile ring method

ground motion, R_L is cyclic triaxial shear stress ratio, r_d is reduction factor of seismic shear stress ration in depth direction, k_{hgL} is design horizontal seismic coefficient, σ_v is total overburden pressure and σ'_v is effective overburden pressure (Referring to Japan road association (2017)).

If the shear stress ratio of the model ground is estimated in terms of effective stress, the horizontal acceleration on the ground surface for $F_L = 1$, which is the condition where liquefaction occurs, is estimated to be 120 gals in Level 1 earthquake (seismic motion of a medium intensity and relatively high probability) and in Type 1 of Level 2 earthquake (large marine earthquake that occurs at the tectonic plate boundaries with low frequency of occurrence), while it is estimated to be 167 gals in Type 2 of Level 2 earthquake (inland earthquake directly below major cities with extremely low frequency of occurrence). This is equivalent to seismic intensity of 5+, if referred to the seismic intensity scale of the Meteorological Agency in Japan.

4. Effect of liquefaction measure of oil tank

During the 1983 Japan Sea Earthquake and the 1995 Hyogo-ken Nanbu Earthquake, settlement and tilting of oil tanks built on reclaimed land were caused by the soil liquefaction. **Photo 1** shows examples of tilted oil tanks caused by the Hyogo-ken Nanbu Earthquake. After this damage of the oil tanks, the Steel Sheet Pile Ring Method was developed as a liquefaction countermeasure. As shown in **Fig. 12** by during steel sheet piles around the tank foundation the shear deformation of the foundation ground can be restrained. This construction method is also effective to prevent lateral flow of liquefied soil.

The effect of this countermeasure on the reduction of tilting and settlement of the tanks was verified in an experiment with a 1:6 scale model. The model used for the experiment is shown in **Fig. 13**. In making the model, the

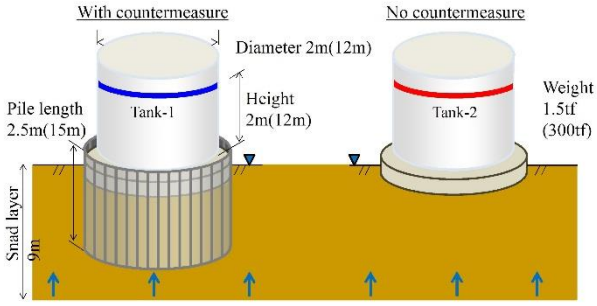

Fig. 13 Model tank

Photo 2. Sloshing (Hamada, 2014)

(a) Before

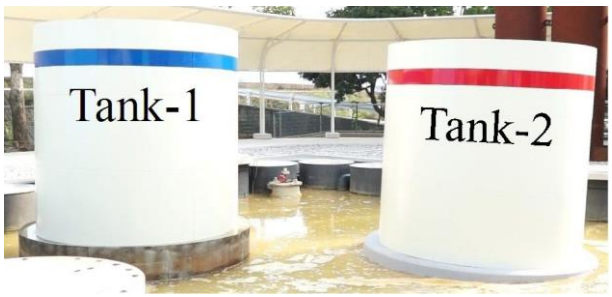

(b) After

Photo 3. Side view

similarity low in the gravity field proposed by Tobita (2016) was referred to. Thin steel plates with creases in polygonal shape were used as steel sheet piles. The thickness of the steel plate was determined to satisfy the similarity low in bending stiffness, and the embedded depth was 2.2 m. A pile toe was set in a liquefiable layer. In the figure, Tank-1 have liquefaction countermeasure, and the steel sheet pile rings and the foundation of the tank were fixed. On the other hand, Tank-2 have no liquefaction countermeasures and were placed directly on the ground surface. In the experiments, a weight was installed to create eccentric load on the bottom slab of the tank, assuming sloshing vibration would occur (**Photo 2**).

Two experiments were carried out with different flow rate Q. Settlement and tilting of the tanks were obtained from the static image (**Photo 3**) filmed during experiments. **Table 2** shows the ratios of settlements and tilting of the tanks with liquefaction countermeasures to those of the tanks without any. The duration of liquefaction in the experiments was set at 10 minutes. In Case-1, the ratios were about 10% for settlements and 0 % for tilting, while they were about 60 % for settlements and 34 % for tilting in Case-2. It is thought that the differences occurred because the upward seepage pressure increased with Q, and the volume increase of the ground was large near the ground surface, it became easier for the settlements and tilting to occur.

Fig. 14 shows the settlement reduction, together with the results of existing researches. Honda (1994 and 1995) and Sakemi *et al.* (1996) simulated the liquefaction countermeasures of the tanks in the results of centrifugal experiments. They embedded the toes of sheet piles installed in a circular configuration into non-liquefiable soil layer. While Kato (2014) conducted centrifuge experiments by shaking table on the effects of the sheet pile wall surrounding house on liquefied ground. On the other hand, in the experiments described in this paper, liquefaction state differs depending on the supplied amount of water as shown in **Fig. 9**. Using excess pore pressures measured at 4 locations, r_u at depths shallower than 6.5 m was estimated by linear interpolation, and the thickness of liquefied layer h was defined for a range of $r_u \fallingdotseq 1$. The embedment ratio during experiments was calculated as the ratio of embedded depth to h and is shown in **Fig. 14** by hollow circles. Though the shapes of the sheet pile configuration are different (rectangular in Kato (2014), and circular in this study), the experimental results obtained here are consistent with what was obtained by Kato (2014) in shaking table experiments, in

which the connection condition between the sheet pile and the tank was relatively similar.

5. Conclusions

From the results of the study, the following summary and conclusions may be drawn:

1) A soil tank was built to simulate hydraulic gradient at the time of ground liquefaction by generating upward seepage water flow in the model ground.
2) It was verified that the strength of the model ground could be maintained constant by controlling the upward water flow.
3) The Steel Sheet Pile Ring Method, a countermeasure against liquefaction, was simulated by a 1:6 scale model in the soil tank, and the pile settlements and inclinations were measured. It was verified that the method had an effect to reduce pile settlements and inclinations even when the steel sheet pile toe was in the liquefiable layer.

In future, liquefaction state will be verified not only by r_u, but by combining it with the change in σ'_v to increase accuracy in the evaluation of ground conditions, and to make use of the results in the development of new liquefaction countermeasures for the evaluation of their effects.

Table 2. Effectiveness of liquefaction countermeasure, settlement and inclination of model tanks

No.	Condition	With countermeasure／No countermeasure	
	Q [m^3/min.]	Settlement	Inclination
Case-1	0.7	0.06	0.00
Case-2	1.3	0.62	0.34

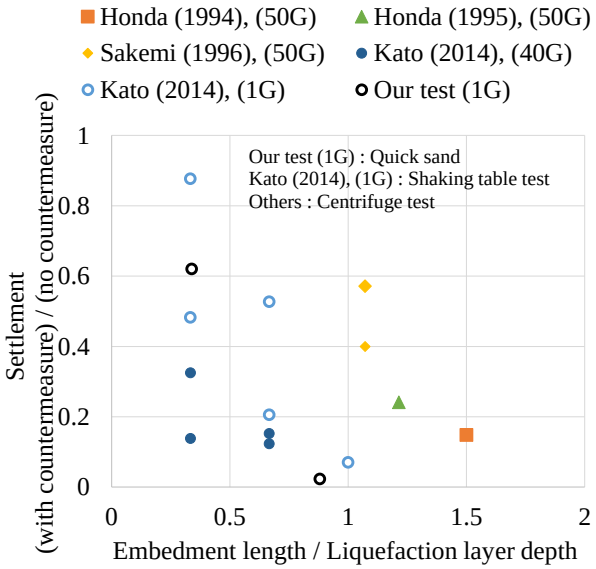

Fig. 14 Effectiveness of liquefaction countermeasure (add to Kato (2014))

References

Hamada, M. 2017. Risks of coastal industrial facilities, Waseda University press. (in Japanese)

Hayashi, K., Fujii, N., Muramatsu, T. and Houjyou, K. 1997. Direct comparison of gravity model and centrifuge model for the seismic problem, Journal of Japan Society of Civil Engineers, Vol. 582, pp. 207-216.

Honda, M., Yamada, T., Hayashi, H. and Katoh, K. 1994. Dynamic centrifuge test on verification of Steel sheet-piles ring foundation method as antiliquefaction measure, Japan National Conference on Geotechnical Engineering, pp. 945-946. (in Japanese)

Honda, M., Obo, N., Yoshizako, K., Katoh, K. 1995. Effectiveness of the steel sheet-piles ring foundation method –Dynamic centrifugal loading experiment test assuming non-contiguous steel sheet-piles ring-, Japan Association for Earthquake Engineering Annual Meeting, Vol. 23, pp. 361-364. (in Japanese)

Ishihara, K. 1998. Basic soil mechanics, Kajima Institute Publishing Co., Ltd. (in Japanese)

The Japanese Geotechnical Society. 2002. Method for axial load test of single piles and commentaries. (in Japanese)

The Japanese Geotechnical Society. 2010. Method for lateral load test of piles and commentaries. (in Japanese)

Japan Road Association. 2017. Specifications for highway bridges Part V: Seismic design. (in Japanese)

The Japanese Geotechnical Society. 1994. Introduction to model experiments in geotechnical engineering, The Japanese Geotechnical Society. (in Japanese)

Kato, I., Hamada, M. Higuchi, S., Kimura, H. and Kimura, Y. 2014. Effectiveness of the sheet pile wall against house subsidence and tilting induced by liquefaction, Journal of Japan Association for Earthquake Engineering, Vol. 14, No.4, pp. 35-49. (in Japanese)

Kusano, K. 1989. Liquefaction-induced ground failures during the 1923 Kanto earthquake in Tokyo lowland, Journal of Japan Society of Civil Engineers, Vol. 406, pp. 213-222. (in Japanese)

Mogami, T., Kubo, K. 1953. The behaviour of soil during vibration, Proceedings of 3rd International Conference on

Soil Mechanics, Vol. 1, pp. 152-155.

Ohne, Y. 2006. Geotechnical engineering, Gihodo shuppan Co., Ltd., pp. 253-257. (in Japanese)

The Ports & Harbours Association of Japan. 2007. Technical standards and commenaries for port and harbor facilities in Japan. (in Japanese)

Sakemi, T., Tanaka, M. and Yuasa, Y. 1996. Settlements of oil storage tank during liquefaction, Journal of Japan Society of Civil Engineers, Vol. 547, pp. 57-65. (in Japanese)

Sangawa, A. 2008. Traces of pale-earthquakes observed at archaeological sites, Journal of Japan Society of Civil Engineers, Ser. C (Geosphere Engineering), Vol. 64, No. 3, pp. 672-679. (in Japanese)

Yasuda, S., 1988. From investigation of liquefaction to countermeasures, Kajima Institute Publishing Co., Ltd. (in Japanese)

Yamashita, A. 1981. The Study of failure process and problems for one-dimensional seepage model tests of sand, 16th Japan National Conference on Geotechnical Engineering, pp. 1117-1120. (in Japanese)

Tani, K. 2013. Suggestions for the use of E-defense to disaster prevention in geotechnical engineering, 58th Geotechnical Symposium, pp. 199-202. (in Japanese)

Tobita, T. 2016. Scaling law and centrifuge modeling in geotechnical engineering, Engineering & Technology, Vol. 23, pp. 11-17. (in Japanese)

Uchida, I., Murata, S. 1981. On the study of shear strength of sand under seepage pressure, Journal of Japan Society of Civil Engineers, Vol. 310. (in Japanese)